Design and Synthesis of Resveratrol-Based Nitrovinylstilbenes as Antimitotic Agents

M. Amarnath Reddy,[†,∥] Nishant Jain,[‡,∥] Deepthi Yada,[†] Chandan Kishore,[‡] Vangala Janakiram Reddy,[‡] P. Surendra Reddy,[†] Anthony Addlagatta,*[‡] Shasi V. Kalivendi,*[‡] and Bojja Sreedhar*[†]

[†]Inorganic and Physical Chemistry Division and [‡]Centre for Chemical Biology, Indian Institute of Chemical Technology (Council of Scientific and Industrial Research), Hyderabad 500607, India

Ⓢ Supporting Information

ABSTRACT: A new series of resveratrol analogues was designed, synthesized, and demonstrated to be tubulin polymerization inhibitors. Most of these compounds exhibited antiproliferative activity and inhibited in vitro tubulin polymerization effectively at concentrations of 4.4−68.1 and 17−62 μM, respectively. Flow cytometry studies showed that compounds **7c**, **7e**, and **7g** arrested cells in the G2/M phase of the cell cycle. Immunocytochemistry revealed loss of intact microtubule structure in cells treated with **7c** and **7e**. Docking of compounds **7c** and **7e** with tubulin suggested that the A-ring of the compounds occupies the colchicine binding site of tubulin, which coordinates with Cys241, Leu242, Ala250, Val318, Val328, and I378, and that the nitrovinyl side chain forms two hydrogen bonds with the main loop of the β-chain at Asn249 and Ala250.
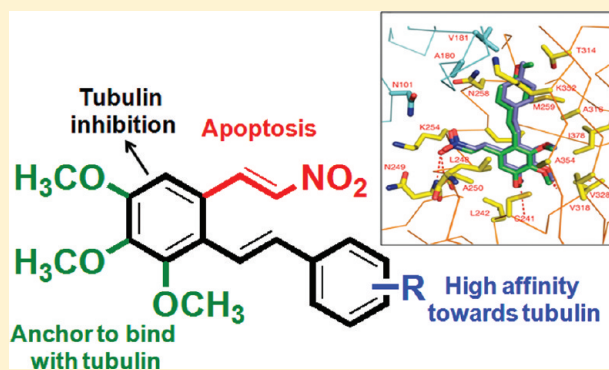
INTRODUCTION

Microtubules are cytoskeletal filaments consisting of α,β-tubulin heterodimers and are involved in a wide range of cellular functions that are critical to the life cycle of the cell.[1] In the mitotic phase of the cell cycle, microtubules are in dynamic equilibrium with tubulin dimers as tubulin is assembled into microtubules, which are disassembled to tubulin. Because inhibition of tubulin polymerization increases the number of cells in metaphase arrest,[2] the interference with the dynamics of tubulin and cell division has been proven to be clinically useful for designing anticancer agents such as paclitaxel,[3] vinblastine,[4] and docetaxel and vincristine.[5]

Resveratrol, **1** ((E)-3,5, 4′-trihydroxystilbene, Figure 1), a polyphenolic stilbene found in the skin of red grapes, various other fruits, and root extract of the plant *Polygonum cuspidatum*, has been an important constituent of Chinese and Japanese folk medicine.[6] Resveratrol has been extensively investigated as a cardioprotective, anti-inflammatory, and antiaging agent.[7] Recent studies have shown that resveratrol has potent anticancer effects. This was evidenced by its in vitro and in vivo inhibitory effects on the growth of a number of tumor cell lines including lymphoma, myeloma, melanoma, breast, pancreatic, colorectal, hepatocellular, and prostate carcinoma.[8] Resveratrol has been reported to have diverse effects on signaling molecules, such as downregulation of the expression of angiogenesis-associated genes, activation of the apoptotic mechanisms,[9] and induction of cell cycle arrest.[10] Resveratrol was also found to sensitize resistant tumor cell lines to a variety of chemotherapeutic agents, such as paclitaxel, thalidomide, and bortezomib.[9]

In view of the great potential of resveratrol as a potent chemotherapeutic agent against a wide variety of cancers, the trihydroxystilbene scaffold of resveratrol has been the subject of synthetic manipulations with the aim of generating novel resveratrol analogues with improved anticancer activity. The *trans*-3,4,5,4′-tetramethoxystilbene analogue, **3** (Figure 1), of **1** has been shown to possess stronger antiproliferative properties than resveratrol in HeLa cervical cancer cells, LnCaP prostate cancer cells, and HepG2 hepatoma cells, as well as HCA-7, HCEC, and HT-29 colon cancer cells.[11]

Compounds having a nitrovinyl side chain attached to the aromatic ring (β-nitrostyrenes) have been reported as proapoptotic anticancer agents, and the nitrovinyl moiety was identified as the pharmacophore for this activity.[12] These compounds have also been described as highly potent and selective inhibitors of human telomerase, by which the essential telomeres that protect chromosomes from exonucleolytic degradation are added to the end of eukaryotic chromosomes.[13] Recently, we have reported nitrovinylbiphenyls as potent cytotoxic agents against a wide range of cancer cell lines.[14] In the present study we report the synthesis and antitumor evaluation of nitrovinylstilbenes that are resveratrol analogues. The *trans*-stilbene

7a = 4-F,   7e = OCH₃,   7i = 4-Br,
7b = 4-Cl,   7f = 3,4,5-(OCH₃)₃, 7j = 4-Ph,
7c = 4-CH₃,   7g = 3,4-Dioxane,   7k = 3,5-(OCH₃)₃
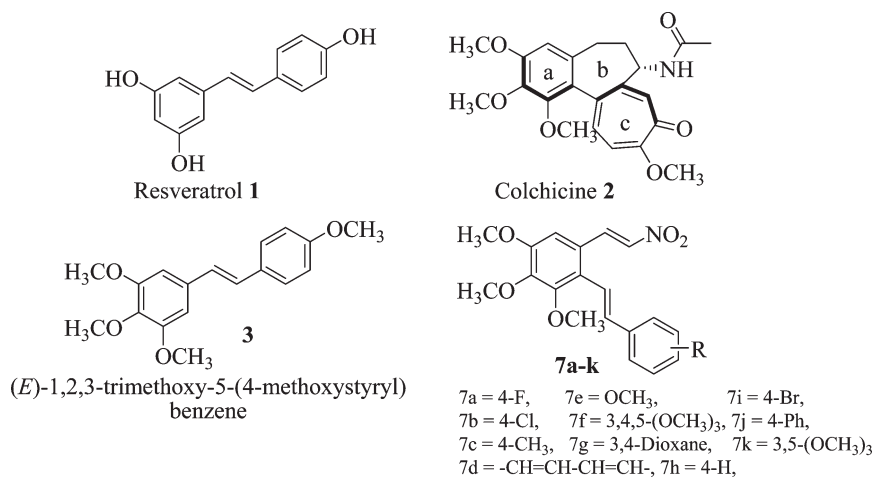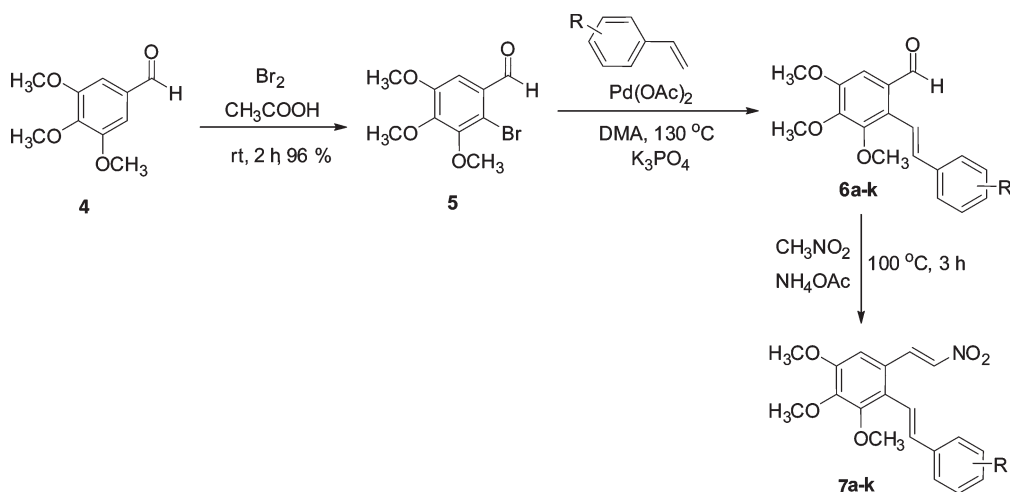7d = -CH=CH-CH=CH-, 7h = 4-H,

Figure 1. Resveratrol and (E)-1,2,3-trimethoxy-5-(4-methoxystyryl)benzene.

Scheme 1. Synthesis of Nitrovinylstilbenes 7a–k, Using Palladium-Catalyzed Heck Coupling

pharmacophore was functionalized with different groups such as methyl, methoxy, methylenedioxy, 3,4,5-trimethoxy, chloro, fluoro, and bromo groups at different positions on compounds with the general formula 7, to furnish derivatives 7a–k.

■ RESULTS AND DISCUSSION

Chemistry. The target 1,2,3-trimethoxy-5-((E)-2-nitrovinyl)-4-styrylbenzenes 7a–k were synthesized as outlined in Scheme 1. 2-Bromo-3,4,5-trimethoxybenzaldehyde 5 was prepared by the bromination of commercially available benzaldehyde 4 with Br₂ at room temperature. The intermediate (E)-3,4,5-trimethoxy-2-styrylbenzaldehydes 6a–k were prepared by reaction of aryl halide 5 with different styrenes in the presence of Pd(OAc)₂. Stilbenes 6a–k were converted to target compounds 7a–k via nitromethane in the presence of ammonium acetate.

In Vitro Cytotoxic Activity. Nitrovinylstilbenes 7a–k were evaluated for their antiproliferative activity against a panel of four different human tumor cells from cervix, breast, lung, and neuroblastoma using the sulforhodamine B assay and were compared with the reference compound resveratrol (1). As shown in Table 1, all of the synthesized compounds possessed

antiproliferative activities against these cell lines in a concentration-dependent manner and were more active than resveratrol. The 4-fluoro (7a), 4-methyl (7c), 4-methoxy (7e), and 3,4-methylenedioxy (7g) derivatives exhibited IC₅₀ values of <12 μM against the HeLa cell line. However, the 4-chloro (7b), 4-bromo (7i), 4-phenyl (7j), and 3,4,5-trimethoxy (7f) derivatives are not active against these cells. The 4-phenyl compound (7j) displayed high cytotoxicity against MCF7 cells, and all other compounds showed moderate potency. In the SK-N-SH cell line, except for 7f and 7h, the derivatives (viz., 7a–k) are more cytotoxic than the control compound 1. Compounds 7c, 7g, and 7k showed antiproliferative activities against A549 cells at concentrations of <20 μM, and 3,4,5-trimethoxy 7f and 7h were active at <30 μM. Of the more active antiproliferative compounds, several are substituted at the 4-position; interestingly, disubstituted derivatives 7g and 7k were similarly effective (Table 1). The compounds were further evaluated by employing more precise biological assays to determine the microtubule-disrupting and antimitotic effects.

Inhibition of in Vitro Tubulin Polymerization. As these hybrid molecules contain a 3,4,5-trimethoxy ring of colchicine, 2 (Figure 1), and a trans-stilbene moiety of resveratrol as the

Table 1. Cytotoxic Effects of Compounds 7a−k and Resveratrol on HeLa, MCF7, A549, and SK-N-SH Human Cancer Cells[a]

7a-k
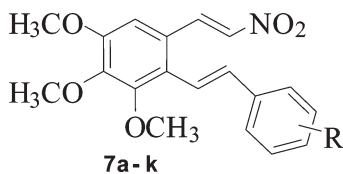
compd	R	IC$_{50}$[b] (pM)			
		MCF-7	SK-N-SH	A549	HeLa
7a	4-F	19.0 ± 0.22	18.8 ± 0.01	35.9 ± 0.10	12.4 ± 0.35
7b	4-Cl	25.7 ± 0.16	12.8 ± 0.1	22.8 ± 0.12	NA
7c	4-CH$_3$	42.5 ± 0.05	12.5 ± 0.16	19.0 ± 0.14	4.4 ± 0.36
7d	−CH=CH—CH=CH−	16.7 ± 0.14	12.0 ± 0.07	59.5 ± 0.08	189.3 ± 0.41
7e	4-OCH$_3$	21.4 ± 0.09	20.7 ± 0.02	40.4 ± 0.09	7.8 ± 0.38
7f	3,4,5-(OCH$_3$)$_3$	13.2 ± 0.15	60.9 ± 0.17	27.1 ± 0.10	NA
7g	3,4-dioxane	19.2 ± 0.09	20.9 ± 0.01	16.3 ± 0.21	5.4 ± 0.17
7h	H	10.9 ± 1.26	68.1 ± 0.21	28.9 ± 0.12	5.42 ± 0.35
7i	4-Br	14.6 ± 0.05	16.6 ± 0.04	41.0 ± 0.07	NA
7j	4-Ph	7.2 ± 0.35	35.8 ± 0.06	44.4 ± 0.06	NA
7k	3,5-(OCH$_3$)$_2$	19.2 ± 0.74	36.2 ± 0.24	15.0 ± 0.69	10 ± 0.25
1	RSV	79.1 ± 0.1	40.3 ± 0.01	44.7 ± 0.06	22.5 ± 0.53

[a] Cell lines were treated with different concentrations of compounds for 48 h as described under Materials and Methods. Cell viability was measured employing SRB assay. [b] IC$_{50}$ values are indicated as the mean ± SD of three independent experiments. NA denotes activity >100 μM.

Table 2. Effect of Compounds 7a−k and Colchicine, 2, on in Vitro Tubulin Polymerization[a]

compd (3 μM)	tubulin polymerization (% inhibition)	compd (3 μM)	tubulin polymerization (% inhibition)
control	0	7f	20
2	58	7g	51
7a	31	7h	31
7b	33	7i	28
7c	62	7j	28
7d	32	7k	27
7e	59	7l	26

[a] Final concentrations of the compounds were 3 μM. The compounds were preincubated with tubulin at a final concentration of 2 mg/mL.

Table 3. Antitubulin Activity of Compounds 7c, 7e, and 7g

compd	IC$_{50}$ (μM)	compd	IC$_{50}$ (μM)
colchicine	1.96 ± 0.2	7e	4.90 ± 0.7
7c	4.27 ± 0.3	7g	8.02 ± 2.6

scaffold, we investigated whether the antiproliferative activities of the compounds (Table 2) were due to their interaction with tubulin by evaluating their antitubulin activity. All of the compounds and standards were employed at a 3 μM final concentration in the assay. To compare, colchicine was used as a positive control (3 μM). The higher cytotoxicity of compounds 7c, 7e, and 7g correlated well with their ability to effectively inhibit tubulin polymerization. In the polymerization assays compound 7c was found to be most active, inhibiting tubulin assembly by 62%, whereas 7e and 7g inhibited tubulin assembly at 59 and 51%, respectively. In comparison, 58% inhibition was observed with colchicine at 3 μM concentration. Interestingly, other compounds of the series that demonstrated lower antiproliferative activities did not possess greater antitubulin activity when compared to standard molecules. Overall, the results suggest that compounds 7c and 7e, which manifested high antiproliferative effects, inhibit tubulin polymerization in vitro and that the

mechanism of action of the compounds other than 7c, 7e, and 7g may not involve tubulin (Table 2). Next, we determined the IC$_{50}$ values of the compounds 7c, 7e, and 7g for their ability to inhibit tubulin assembly. As expected, compound 7c, which demonstrated the maximum inhibition of tubulin assembly, manifested the lowest IC$_{50}$ (4.27 μM). However, compounds 7e and 7g demonstrated IC$_{50}$ values of 4.9 and 8.2 μM, respectively (Table 3). The obtained results support the findings that the compounds inhibit tubulin assembly in the order 7c > 7e > 7g.

Antimitotic Effects of Active Compounds. To determine whether the cytotoxic effects induced by the treatment of these nitrovinylstilbene derivatives were due to cell cycle arrest, we performed flow cytometry analysis. HeLa cells were treated with compounds 7c, 7e, and 7g at concentrations of 5 μM for a duration of 24 h. Later, cells were harvested and analyzed by flow cytometry. Interestingly, major populations of cells treated with compounds 7c and 7e arrested at the G2/M phase with 66 and 60% accumulation, respectively (Figure 2 and Table 4), and cells treated with 7g showed significant arrest at the G2/M phase (50%). These results confirm the growth inhibitory effects of these nitrovinylstilbene derivatives 7c and 7e on cervical cancer cells.

Effects of 7c and 7e on Cellular Microtubules and Nuclear Morphology. We examined the morphology of HeLa cells treated with 7c and 7e at 5 μM concentrations for 24 h. After 24 h, cells were fixed and stained with antitubulin antibody.
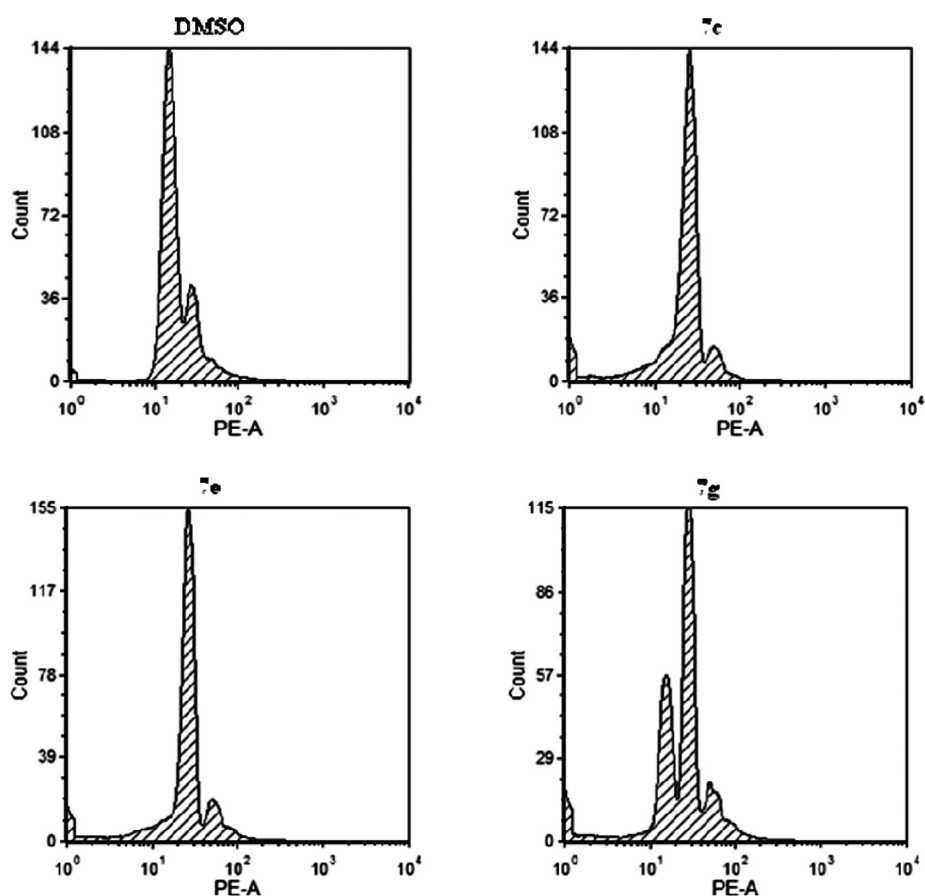
Figure 2. Antimitotic effects of **7c**, **7e**, and **7g** by FACS analysis. HeLa cells were harvested after treatment at 5 μM concentration of **7c**, **7e**, and **7 g** for 24 h. Untreated cells and DMSO-treated cells served as controls. Cell cycle analysis was performed employing propidium iodide as indicated underMaterials and Methods. The percentage of cells in each phase of cell cycle was quantified by flow cytometry.

Table 4. Distribution of Cells at G1 and G2/M Phase of Cell Cycle following Treatment with 7c, 7e, and 7g in HeLa Cells[a]

compd	% of cells in G1 phase	% of cells in S phase	% of cells in G2/M phase
control	69.43	9.28	21.29
7c	9.66	23.91	66.43
7e	16.64	22.96	60.40
7g	27.14	22.30	50.56

[a] Cell cycle analysis was performed after treatment of cells with **7c**, **7e**, and **7g** using flow cytometry. HeLa cells were treated with 5 μM concentration of **7c**, **7e**, and **7g** for 24 h and subjected to cell cycle analysis following staining with propidium iodide as mentioned under Materials and Methods.

4′,6-Diamidino-2-phenylindole (DAPI) was used to stain the nucleus. The microtubule network was normal in the control cells, whereas HeLa cells treated with nitrovinylstilbenes **7c** and **7e** demonstrated disrupted microtubule networks, having normal bipolar spindles but incomplete chromosome separation: a majority of plane, indicating an arrest at metaphase (Figure 3).

Activation of Caspase-3. Cells arrested at mitosis undergo cell death in a caspase-dependent manner, due to spindle poison-induced mitotic catastrophe or resulting from the improper segregation of chromosomes, delayed mitosis, and abortive centrosome duplications[15] leading to the activation of caspase-3.

We examined the activation of caspase-3 in HeLa cells treated for 24 h at 1 and 5 μM concentrations with compounds **7c** and **7e**. Resveratrol (**1**) was also used at the same concentrations for comparison. Compound **7c** treatments resulted in a 12-fold increase in caspase-3 activity at 5 μM concentration. In contrast, resveratrol did not induce any significant increase in caspase-3 activation at 5 μM concentration. However, at much higher concentrations of **1** (40 μM), a 5−8-fold increase in caspase-3 activity was found (data not shown). Cells treated with 5 μM compound **7e** showed a 10-fold induction in caspase-3 activity (Figure 4). In conclusion, compounds **7c** and **7e** activated caspase-3 at much lower concentrations than resveratrol.

Docking Results. The hybrid molecules in the present study were designed on the basis of the trimethoxyphenyl group from colchicine, which occupies the colchicine binding pocket of tubulin. To elucidate their mode of binding with tubulin and consequent microtubule formation, we examined whether the selected compounds **7c** and **7e** directly dock to the colchicine binding site of β-tubulin. Autodock results suggest that the docking position of the trimethoxyphenyl group of compounds **7c** and **7e** showed a similar binding mode to that of the A-ring of colchicine, making extensive hydrophobic contacts with the binding pocket of the β-chain (Figure 5A). Some of the amino acids in contact with the A-ring of the trimethoxyphenyl group are Cys241, Leu242, Ala250, Val318, Val328, and I378. In addition to the good hydrophobic contacts, the nitrovinyl group
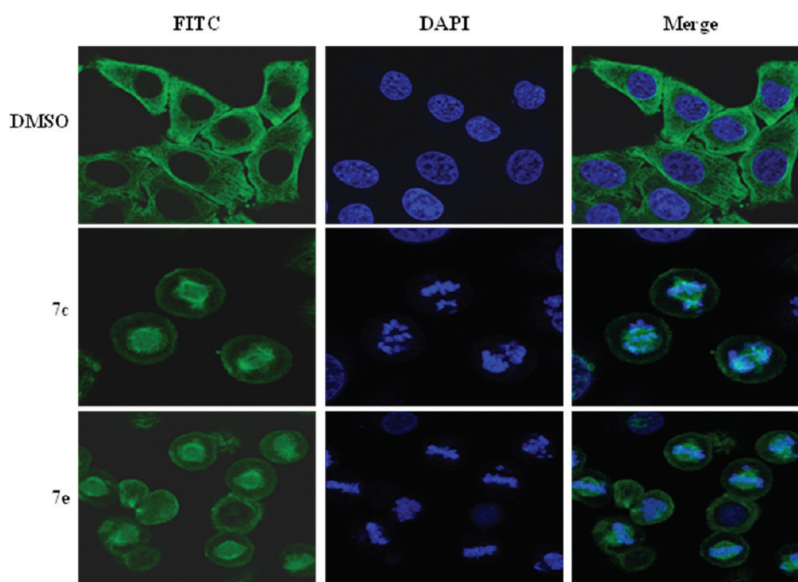
Figure 3. Effect of **7c** and **7e** on microtubule organization and nuclear condensation. HeLa cells were independently treated with **7c** and **7e** at 5 μM concentration for 24 h. Following the termination of the experiment, cells were fixed and stained for tubulin. DAPI was used as counter stain. The merged images of cells stained for tubulin and DAPI are represented. The photographs were taken using an Olympus confocal microscope equipped with FITC and DAPI filter settings. Data are representative of five different fields of view.
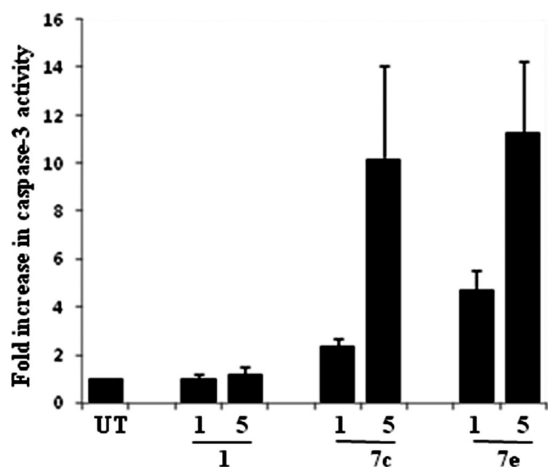

Figure 4. Effect of different concentrations of resveratrol and compounds **7c** and **7e** on caspase-3 activity in HeLa cells. Following the termination of incubation, caspase-3 activity from cellular lysate was monitored by fluorometry as described under Materials and Methods. Data represent the mean $\pm$ SD of three different experiments.

extends to the nearby main-chain loop of the β-chain at Asn249 and Ala250, forming two hydrogen bonds (3.2 and 2.8 Å) (Figure 5B). These interactions appear to be very significant in the binding of this new series of molecules. The B-ring in the stilbene moiety extends into the interface of the $\alpha\beta$-chains of tubulin. Our aim was to vary the substitutions on this B-ring so that they selectively inhibit formation of the α,β-dimer. 4-Methyl and 4-methoxy groups appear to have more selectivity for binding in this interface compared to other substitutions. Moreover, V181, Thr314, and K352 also are critical in the structure−activity relationship displayed by the series of compounds. Surprisingly, isostructural halogen substituents do not show similar affinity. Other substitutions such as phenyl and naphthyl

did not yield a suitable position in the docking simulations due to steric hindrance.

■ CONCLUSION

In the present study, we performed the synthesis and biological evaluation of synthetic antitubulin compounds 1,2,3-trimethoxy-5-((E)-2-nitrovinyl)-4-styrylbenzene derivatives (**7a**−**k**) based on **1** and **2** (Figure 1). A majority of these compounds demonstrated significant antiproliferative activity against the cancer cell lines tested. We have identified two compounds, **7c** and **7e**, as potent antiproliferative agents and inhibitors of tubulin polymerization. Similar to other antitubulin agents, **7c** and **7e** induced cell cycle arrest at the G2/M phase. Treatment of cells with compounds **7c** and **7e** resulted in the formation of bipolar spindles, indicating a metaphase arrest. The docking position of the trimethoxyphenyl group of compounds **7c** and **7e** exhibited a binding mode similar to that of the A-ring of colchicine. Hence, the compounds of this structural class are amenable to further modifications and will be useful as templates for the design of new anticancer agents.

■ MATERIALS AND METHODS

Biology. Materials and Methods. Cell Culture and Maintenance. All cell lines used in this study were purchased from the American Type Culture Collection (ATCC). A549 (human lung carcinoma epithelial), SK-N-SH (human neuroblastoma), and HeLa (human epithelial cervical cancer) were grown in Dulbecco's modified Eagle's medium (containing 10% FBS in a humidified atmosphere of 5% CO_2 at 37 °C). MCF-7 (human breast adenocarcinoma) cells were cultured in Eagle's minimal essential medium (MEM) containing nonessential amino acids, 1 mM sodium pyruvate, 10 mg/mL bovine insulin, and 10% FBS. Cells were trypsinized when subconfluent from T75 flasks/90 mm dishes and seeded in 12- or 6-well plates at a concentration of 2.5×10^5 cells/mL in complete medium, treated with compounds at desired concentrations for 48 h, and
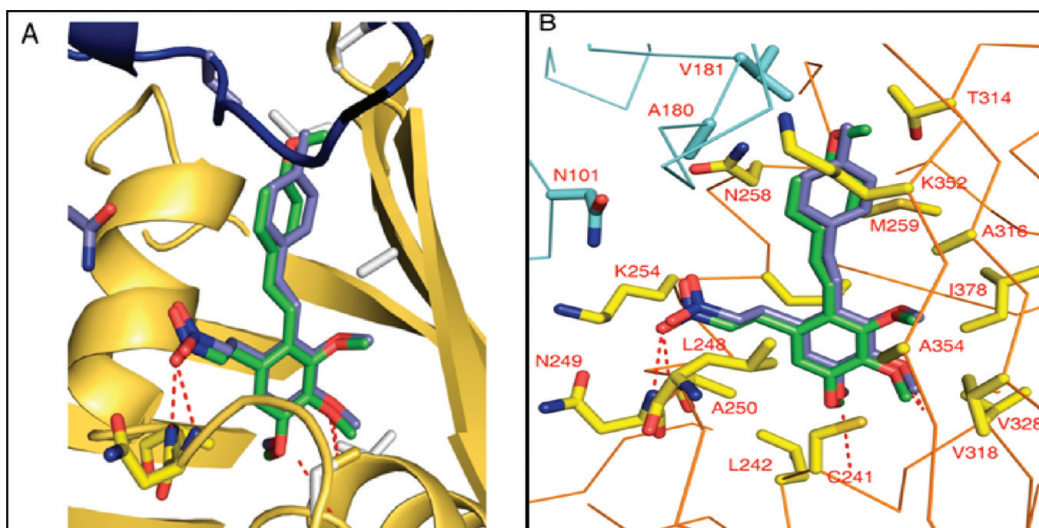
Figure 5. Binding of compounds **7c** (blue sticks) and **7e** (green sticks) with the $\alpha\beta$-interface of tubulin. Note that the trimethoxyphenyl ring (ring A) of both compounds docks well in the crevice of the β-chain (gold) whereas the nitrovinyl also makes contact with Asn249 and Ala250 main-chain amide nitrogen atoms. The B-ring of stilbene extends into the $\alpha\beta$-interface.

harvested as required. For immunohistochemistry experiments, wells were seeded on coverslips in a 6-well plate.

Antiproliferative Assays. The synthesized compounds (**7a**–**k**) were evaluated for their in vitro cytotoxicity in four different human cancer cell lines. A protocol of 48 h continuous drug exposure was used, and a sulforhodamine B (SRB) protein assay was used to estimate cell viability or growth. The cell lines were grown in their respective media containing 10% fetal bovine serum and 2 μM L-glutamine and were inoculated into 96-well microtiter plates in 90 μL aliquots at plating densities depending on the doubling time of individual cell lines. The microtiter plates were incubated at 37 °C, in 5% CO_2/95% air, and at 100% relative humidity for 24 h prior to addition of experimental drugs. Aliquots of 10 μL of the drug dilutions were added to the appropriate microtiter wells already containing 90 μL of cells, resulting in the required final drug concentrations. For each compound, four concentrations (0.1, 1, 10, and 100 μM) were evaluated, and each was done in triplicate wells. Plates were incubated further for 48 h, and the assay was terminated by the addition of 50 μL of cold trichloroacetic acid (TCA) (final concentration = 10% TCA) and incubation for 60 min at 4 °C. The plates were washed five times with tap water and air-dried. SRB solution (50 μL) at 0.4% (w/v) in 1% acetic acid was added to each of the wells, and plates were incubated for 20 min at room temperature. The residual dye was removed by washing five times with 1% acetic acid. The plates were air-dried. Bound stain was subsequently eluted with 10 μM Trizma base, and the absorbance was read on a multimode plate reader at a wavelength of 540 nm with 690 nm reference wavelengths. Percent growth was calculated on a plate by plate basis for test wells relative to control wells. The above determinations were repeated three times. The growth inhibitory effects of the compounds were analyzed by generating dose-response curves as a plot of the percentage of surviving cells versus drug concentration. Sensitivity of the cancer cells to the drug treatment was expressed in terms of IC_{50}, a value defined as the concentration of compound that produced 50% reduction as compared to the control absorbance.[16] The percentage of cells killed was obtained from the following formula:

$$\% \text{ of cells killed} = \frac{100 - \text{meanOD}_{\text{sample}}}{\text{meanOD}_{\text{day0}}} \times 100$$

Analysis of Cell Cycle. Human cervical cancer cells (HeLa) in 60 mm dishes were incubated for 24 h in the presence or absence of test

compounds **7c**, **7g**, and **7e** (5 μM). Cells were harvested with trypsin—ethylenediaminetetraacetic acid (EDTA) and fixed with ice-cold 70% ethanol at 4 °C for 30 min; ethanol was removed by centrifugation, and cells were stained with 1 mL of DNA staining solution (0.2 mg of propidium iodide (PI) and 2 mg of RNase A) for 30 min as described earlier. The DNA contents of 20000 events were measured by flow cytometry (BD FACSCanto II). Histograms were analyzed using FCS express 4 plus.[16]

Tubulin Polymerization Assay. An in vitro assay for monitoring the time-dependent polymerization of tubulin to microtubules was performed employing a fluorescence-based tubulin polymerization assay kit (BK011, Cytoskeleton, Inc.) according to the manufacturer's protocol. The reaction mixture in a final volume of 10 μL in PEM buffer (80 mM PIPES, 0.5 mM ethylene glycol tetraacetic acid (EGTA), 2 mM $MgCl_2$, pH 6.9) contained 2 mg/mL bovine brain tubulin, 10 μM fluorescent reporter, and 1 mM guanosine triphosphate (GTP) in the presence or absence of test compounds (3 μM final concentration) at 37 °C. Tubulin polymerization was followed by monitoring the fluorescence enhancement due to the incorporation of a fluorescence reporter into microtubules as polymerization proceeded. Fluorescence emission at 420 nm (excitation wavelength is 360 nm) was measured for 1 h at 1 min intervals in a multimode plate reader (Tecan M200). Nocodazole and colchicine were used as positive controls under similar experimental conditions. To determine the IC_{50} values of the compounds against tubulin polymerization, the compounds were preincubated with tubulin at various concentrations (1, 2, 3, 4, and 5 μM). Assays were performed under conditions similar to those employed for the polymerization assays described above.[17]

Immunohistochemistry of Tubulin and Analysis of Nuclear Morphology. HeLa cells were seeded on glass coverslips and incubated for 24 h in the presence or absence of test compounds **7c** and **7e** (5 μM). Cells grown on coverslips were fixed in 3.5% formaldehyde in phosphate-buffered saline (PBS), pH 7.4, for 10 min at room temperature. Cells were permeablized for 6 min in PBS containing 0.5% Triton X-100 (Sigma) and 0.05% Tween-20 (Sigma). The permeablized cells were incubated with 2% bovine serum albumin (BSA) (Sigma) in PBS for 1 h for blocking. Later, the cells were incubated with primary antibodies diluted in blocking solution for 4 h at room temperature. Subsequently, the antibodies were removed and the cells were washed with PBS three times. Cells were then incubated with

secondary antibodies for 1 h at room temperature. The cells were washed three times with PBS and mounted in medium containing DAPI. Images were captured using the Olympus camera and analyzed with Provision software.[18]

Caspase-3 Assay. HeLa cells in 6-well plates were grown to 60−80% confluence and treated with either no drug or two concentrations of resveratrol, **7c**, and **7g** (1 and 5 μM). After 24 h, cells were collected by scraping, washed with PBS, and centrifuged at 3000 rpm for 1 min at 4 °C to collect pellet. Later, cells were lysed in 200 μL of 1× lysis buffer followed by incubation on ice for 10−20 min. The lysate was centrifuged at 13200 rpm for 20 min at 4 °C to collect the pellet, and the clear supernatant was used for caspase activity measurements employing amido-4-methylcoumarin (AMC) conjugated substrates for caspase-3 as described earlier.[18]

Methodology. Docking was carried out by AutoDock4,[19] in the predefined colchicine binding domain.[20] The Grid map in Autodock that defines the interaction of protein and ligands in the binding pocket was defined. The grid map was used with 55 points in each x, y, and z direction, equally spaced at 0.375 Å. Docking was performed using the Lamarckian genetic algorithm in AutoDock4.[21] Each docking experiment was performed 10 times, yielding 10 docked conformations. Parameters used for the docking were as follows: population size of 150; random starting position and conformation; maximal mutation of 2 Å in translation and 50° in rotations; elitism of 1; mutation rate of 0.02 and crossover rate of 0.8; and local search rate of 0.06. Simulations were performed with a maximum of 1.5 million energy evaluations and a maximum of 27000 generations. Final docked conformations were clustered using a tolerance of 1 Å root-mean-square deviation (rmsd). The best model was picked on the basis of the best stabilization energy.

■ EXPERIMENTAL SECTION

Chemistry. *Materials and Methods.* All chemicals were purchased from Sigma-Aldrich and SD Fine Chemicals, Pvt. Ltd. India, and used as received. ACME silica gel (100−200 mesh) was used for column chromatography, and thin-layer chromatography was performed on Merck-precoated silica gel 60-F_{254} plates. All other chemicals and solvents were obtained from commercial sources and purified using standard methods. The IR spectra of all compounds were recorded on a Perkin-Elmer Spectrum GX FTIR spectrometer. The IR values are reported in reciprocal centimeters (cm^{-1}). The ^{1}H and ^{13}C NMR spectra were recorded on a Bruker-Avance 300 MHz spectrometer (see the Supporting Information). Chemical shifts (δ) are reported in parts per million, using TMS ($\delta = 0$) as an internal standard in CDCl$_3$. ESI mass spectra were recorded on a Finnigan LCQ Advantagemax spectrometer. High-resolution mass spectra (HRMS) were recorded on a QSTAR XL Hybrid MS/MS mass spectrometer. All products reported showed ^{1}H NMR and ^{13}C NMR spectra in agreement with the assigned structures. The purity of compounds was determined by HRMS, and all tested compounds yielded data consistent with a purity of at least 95% compared with the theoretical values.

Synthesis of 2-Bromo-3,4,5-trimethoxybenzaldehyde (5). A 500 mL round-bottom flask was charged with 3,4,5-trimethoxybenzaldehyde **4** (5.00 g, 25.5 mmol), methylene chloride (100 mL), and acetic acid (200 μL). The flask was cooled to 0 °C in an ice bath, and bromine (1.31 mL, 25.5 mmol) in methylene chloride (10 mL) was added dropwise via an addition funnel over 15 min. After 30 min of stirring at 0 °C, aqueous sodium thiosulfate was added, and the mixture was extracted three times with methylene chloride. The combined organic layers were washed with saturated aqueous sodium bicarbonate and brine and dried over sodium sulfate. Removal of the solvent under reduced pressure gave a solid, which was recrystallized from ethyl acetate/hexane (EtOAc/hexane) to give **5** (6.37 g, 31.1 mmol, 91%) as colorless needles: mp 67−69 °C; IR (neat) 2981, 1690, 1579, 1481,

1385, 1286, 1199, 1166, 1045, 922 cm^{-1}; ^{1}H NMR (300 MHz, CDCl$_3$) δ 3.91 (s, 3H), 3.92 (s, 3H), 3.99 (s, 3H), 7.32 (s, 1H), 10.13 (s, 1H); ^{13}C NMR (75 MHz, CDCl$_3$) δ 56.2, 61.1, 61.2, 107.4, 115.6, 128.8, 148.7, 150.6, 152.9, 190.9.

General Procedure A for the Synthesis of Stilbenes 6a−k. To a mixture of aryl halide **5** (1.0 equiv) and styrene (1.2 equiv) into dimethylacetamide (DMA, 3 mL) in a 50 mL round-bottom flask were added 3 mol % Pd(OAc)$_2$ and 1.5 equiv of K$_3$PO$_4$, and the reaction mixture was subjected to reflux at 150 °C for 12 h. Reaction was monitored by TLC and purified by column chromatography.

(E)-2-(4-Fluorostyryl)-3,4,5-trimethoxybenzaldehyde (6a). Following general procedure A, compound **6a** was purified by column chromatography, eluting with hexane/EtOAc (9.7:0.3): 96% yield; pale yellow solid; mp 83−86 °C; IR (KBr) v 2937, 1686, 1588, 1485, 1334, 1125, 1071, 984 cm^{-1}; ^{1}H NMR (300 MHz, CDCl$_3$) δ 3.86 (s, 3H), 3.95 (s, 6H), 6.58 (d, 1H, $J = 16.2$ Hz), 7.01−7.09 (m, 2H), 7.24−7.33 (m, 2H), 7.45−7.53 (m, 2H), 10.10 (s, 1H); ^{13}C NMR (75 MHz, CDCl$_3$) δ 56.0, 61.0, 106.6, 115.6, 115.8, 119.0, 128.2, 128.4, 129.9, 130.3, 133.0, 136.9, 161.0, 164.3, 190.9; ESI MS (m/z) 317 (M + H).

(E)-2-(4-Chlorostyryl)-3,4,5-trimethoxybenzaldehyde (6b). Following general procedure A, compound **6b** was purified by column chromatography, eluting with hexane/EtOAc (9.6:0.4): 91% yield; pale yellow solid; mp 78−81 °C; IR (KBr) v 2924, 2850, 1680, 1585, 1487, 1331, 1124, 1075, 983 cm^{-1}; ^{1}H NMR (300 MHz, CDCl$_3$) δ 3.86 (s, 3H), 3.95 (s, 6H), 6.58 (d, 1H, $J = 15.8$ Hz), 7.26 (s, 1H), 7.3−7.4 (m, 3H), 7.45 (d, 2H, $J = 8.3$ Hz), 10.09 (s, 1H); ^{13}C NMR (75 MHz, CDCl$_3$) δ 56.1, 61.0, 106.7, 120.0, 127.9, 128.9, 129.9, 130.0, 133.9, 135.2, 136.7, 146.9, 151.6, 152.9, 190.8; ESI MS (m/z) 333 (M + H).

(E)-3,4,5-Trimethoxy-2-(4-methylstyryl)benzaldehyde (6c). Following general procedure A, compound **6c** was purified by column chromatography, eluting with hexane/EtOAc (9.5:0.5): 97% yield; pale yellow solid; mp 79−82 °C; IR (KBr) v 2919, 2850, 1737, 1637, 1461, 1372, 1241, 1123, 1026 cm^{-1}; ^{1}H NMR (300 MHz, CDCl$_3$) δ 2.38 (s, 3H), 3.85 (s, 3H), 3.95 (s, 6H), 6.56 (d, 1H, $J = 16.2$ Hz), 7.15 (d, 2H, $J = 7.9$ Hz), 7.26 (s, 1H), 7.30 (d, 1H, $J = 16.2$ Hz), 7.40 (d, 2H, $J = 7.9$ Hz), 10.10 (s, 1H); ^{13}C NMR (75 MHz, CDCl$_3$) δ 21.2, 56.0, 61.0, 106.4, 118.2, 126.6, 129.4, 129.9, 133.8, 134.0, 138.3, 147.0, 149.9, 151.6, 152.7, 191.0; ESI MS (m/z) 313 (M + H).

(E)-3,4,5-Trimethoxy-2-(2-(naphthalen-2-yl)vinyl)benzaldehyde (6d). Following general procedure A, compound **6d** was purified by column chromatography, eluting with hexane/EtOAc (9.6:0.4): 96% yield; pale yellow solid; mp 89−91 °C; IR (KBr) v 2925, 2854, 1677, 1582, 1486, 1335, 1125, 1030, 986 cm^{-1}; ^{1}H NMR (300 MHz, CDCl$_3$) δ 3.89 (s, 3H), 3.96 (s, 6H), 6.79 (d, 1H, $J = 15.9$ Hz), 7.28 (s, 1H), 7.42−7.54 (m, 3H), 7.75−7.85 (m, 5H), 10.17 (s, 1H); ^{13}C NMR (75 MHz, CDCl$_3$) δ 56.0, 61.0, 106.6, 119.6, 123.3, 126.3, 126.4, 127.2, 127.7, 128.0, 128.4, 130.0, 130.6, 133.2, 133.5, 134.2, 138.3, 147.0, 151.7, 152.8, 190.9; ESI MS (m/z) 349 (M + H).

(E)-3,4,5-Trimethoxy-2-(4-methoxystyryl)benzaldehyde (6e). Following general procedure A, compound **6e** was purified by column chromatography, eluting with hexane/EtOAc (9.4:0.6): 92% yield; pale yellow solid; mp 98−101 °C; IR (KBr) v 2928, 2851, 1677, 1595, 1479, 1336, 1122, 1029, 979 cm^{-1}; ^{1}H NMR (300 MHz, CDCl$_3$) δ 3.85 (s, 6H), 3.95 (s, 6H), 6.53 (d, 1H, $J = 16.2$ Hz), 6.86 (d, 2H, $J = 8.7$ Hz), 7.21 (d, 1H, $J = 16.2$ Hz), 7.25 (s, 1H), 7.44 (d, 2H, $J = 8.7$ Hz), 10.10 (s, 1H); ^{13}C NMR (75 MHz, CDCl$_3$) δ 55.3, 56.0, 61.0, 106.3, 114.1, 117.0, 128.0, 129.6, 129.9, 131.0, 137.9, 146.9, 151.5, 152.6, 159.8, 191.0; ESI MS (m/z) 329 (M + H).

(E)-3,4,5-Trimethoxy-2-(3,4,5-trimethoxystyryl)benzaldehyde (6f). Following general procedure A, compound **6f** was purified by column chromatography, eluting with hexane/EtOAc (9.2:0.8): 84% yield; pale yellow solid; mp 103−105 °C; IR (KBr) v 2943, 2849, 1676, 1581, 1457, 1335, 1124, 1076, 963 cm^{-1}; ^{1}H NMR (300 MHz, CDCl$_3$) δ 3.84 (s, 3H), 3.86 (s, 3H), 3.91 (s, 6H), 3.95 (s, 6H), 6.52 (d, 1H,

$J = 16.6$ Hz), 6.71 (s, 2H), 7.23−7.29 (m, 2H), 10.10 (s, 1H); ^{13}C NMR (75 MHz, CDCl$_3$) δ 56.1, 60.9, 61.1, 103.8, 106.5, 118.7, 127.9, 130.0, 130.4, 132.4, 134.7, 138.2, 147.0, 151.6, 152.8, 153.4, 190.1; ESI MS (m/z) 389 (M − H).

(E)-2-(2-(Benzo[d][1,3]dioxol-5-yl)vinyl)-3,4,5-trimethoxybenzaldehyde (6g). Following general procedure A, compound **6g** was purified by column chromatography, eluting with hexane/EtOAc (9.4:0.6): 96% yield; pale yellow solid; mp 64−68 °C; IR (KBr) v 2934, 1667, 1580, 1488, 1251, 1129, 1035, 969 cm^{-1}; ^{1}H NMR (300 MHz, CDCl$_3$) δ 3.85 (s, 3H), 3.94 (s, 6H), 5.98 (s, 2H), 6.50 (d, 1H, $J = 16.1$ Hz), 6.77 (d, 1H, $J = 7.9$ Hz), 6.92 (d, 1H, $J = 7.9$ Hz), 7.07 (s, 1H), 7.18 (d, 1H, $J = 16.1$ Hz), 7.24 (s, 1H), 10.08 (s, 1H); ^{13}C NMR (75 MHz, CDCl$_3$) δ 56.0, 61.0, 101.2, 105.6, 106.4, 108.4, 117.4, 122.0, 129.9, 130.7, 131.3, 134.4, 137.9, 147.8, 148.2, 151.5, 152.7, 190.1; ESI MS (m/z) 343 (M + H).

(E)-3,4,5-Trimethoxy-2-styrylbenzaldehyde (6h). Following general procedure A, compound **6h** was purified by column chromatography, eluting with hexane/EtOAc (9.5:0.5): 92% yield; pale yellow solid; mp 76−78 °C; IR (KBr) v 2938, 2850, 1680, 1585, 1486, 1333, 1125, 1072 cm^{-1}; ^{1}H NMR (300 MHz, CDCl$_3$) δ 3.86 (s, 3H), 3.95 (s, 6H), 6.60 (d, 1H, $J = 16.2$ Hz), 7.23−7.30 (m, 2H), 7.31−7.40 (m, 3H), 7.51 (d, 2H, $J = 7.4$ Hz), 10.12 (s, 1H); ^{13}CNMR (75 MHz, CDCl$_3$) δ 56.0, 61.0, 106.4, 119.3, 126.7, 128.2, 128.7, 129.9, 130.5, 136.7, 138.2, 146.9, 151.6, 152.8, 190.9; ESI MS (m/z) 299 (M + H).

(E)-2-(4-Bromostyryl)-3,4,5-trimethoxybenzaldehyde (6i). Following general procedure A, compound **6i** was purified by column chromatography, eluting with hexane/EtOAc (9.4:0.6): 92% yield; pale yellow solid; mp 102−104 °C; IR (KBr) v 2925, 2854, 1678, 1582, 1484, 1333, 1124, 1068, 962 cm^{-1}; ^{1}H NMR (300 MHz, CDCl$_3$) δ 3.86 (s, 3H), 3.96 (s, 6H), 6.57 (d, 1H, $J = 15.8$ Hz), 7.33−7.34 (m, 4H), 7.49 (d, 2H, $J = 9.0$ Hz), 10.09 (s, 1H); ^{13}C NMR (75 MHz, CDCl$_3$) δ 56.0, 61.0, 106.8, 120.2, 122.1, 127.1, 128.1, 129.9, 131.8, 135.7, 136.7, 147.0, 151.7, 153.0, 190.7; ESI MS (m/z) 401 (M + Na).

(E)-2-(2-(Biphenyl-4-yl)vinyl)-3,4,5-trimethoxybenzaldehyde (6j). Following general procedure A, compound **6j** was purified by column chromatography, eluting with hexane/EtOAc (9.4:0.6): 93% yield; pale yellow solid; mp 85−89 °C; IR (KBr) v 2933, 2852, 1677, 1582, 1485, 1333, 1122, 1069, 984 cm^{-1}; ^{1}H NMR (300 MHz, CDCl$_3$) δ 3.87 (s, 3H), 3.96 (s, 6H), 6.65 (d, 1H, $J = 16.2$ Hz), 7.27 (s, 1H), 7.30−7.63 (m, 10H), 10.14 (s, 1H); ^{13}C NMR (75 MHz, CDCl$_3$) δ 56.1, 61.0, 106.5, 119.4, 126.9, 127.2, 127.4, 128.7, 129.3, 130.0, 130.6, 134.7, 135.7, 137.8, 140.4, 141.0, 151.6, 152.8, 190.9; ESI MS (m/z) 375 (M + H).

(E)-2-(3,5-Dimethoxystyryl)-3,4,5-trimethoxybenzaldehyde (6k). Following general procedure A, compound **6k** was purified by column chromatography, eluting with hexane/EtOAc (9.3:0.7): 95% yield; pale yellow solid; mp 60−62 °C; IR (KBr) v 2936, 2844, 1679, 1590, 1460, 1332, 1125, 1067, 988 cm^{-1}; ^{1}H NMR (300 MHz, CDCl$_3$) δ 3.82 (s, 6H), 3.86 (s, 3H), 3.94 (s, 3H), 3.96 (s, 3H), 6.38 (s, 1H), 6.53 (d, 1H, $J = 16.2$ Hz), 6.63 (s, 2H), 7.27 (s, 1H), 7.33 (d, 1H, $J = 16.2$ Hz), 10.10 (s, 1H); ^{13}C NMR (75 MHz, CDCl$_3$) δ 55.4, 56.1, 61.0, 100.5, 104.8, 106.5, 106.9, 119.9, 121.3, 130.0, 130.3, 138.2, 138.7, 152.9, 161.0, 190.9; ESI MS (m/z) 359 (M + H).

General Procedure B for the Synthesis of Nitrovinylstilbenes 7a−k. A mixture of biphenyl **6** (0.5 mmol) and ammonium acetate (1 mmol, 2 equiv) in nitromethane (2 mL) was stirred at 100 °C for 2 h. After completion of the reaction as indicated by TLC, the reaction mixture was diluted with water and extracted with EtOAc (2 × 10 mL). The combined organic layers were dried over anhydrous sodium sulfate, concentrated in vacuo, and purified by column chromatography on silica gel using hexane/EtOAc as eluent, to afford the pure product **7**.

2-(4-Fluorostyryl)-3,4,5-trimethoxy-1-((E)-2-nitrovinyl)benzene (7a). Following general procedure B, compound **7a** was purified by column chromatography, eluting with hexane/EtOAc (9.6:0.4): 80% yield; yellow solid; mp 108−110 °C; IR (KBr) v 2930, 1623, 1593, 1483, 1083 cm^{-1}; ^{1}H NMR (300 MHz, CDCl$_3$) δ 3.86 (s, 3H), 3.93 (s, 6H), 6.53 (d, 1H, $J = 16.4$ Hz), 6.78 (s, 1H), 7.01−7.11 (m, 2H), 7.16 (d, 1H, $J = 16.4$ Hz), 7.42−7.52 (m, 3H), 8.30 (d, 1H, $J = 13.6$ Hz); ^{13}C NMR (75 MHz, CDCl$_3$) δ 56.2, 61.0, 61.1, 106.5, 115.6, 115.9, 121.0, 123.7, 128.2, 128.3, 133.1, 136.3, 137.0, 138.4, 145.3, 152.1, 152.9; ESI MS (m/z) 360 (M + H); HRMS (ESI) (m/z) calcd for C$_{19}$H$_{19}$NO$_5$F, 360.1247, found, 360.1232.

2-(4-Chlorostyryl)-3,4,5-trimethoxy-1-((E)-2-nitrovinyl)benzene (7b). Following general procedure B, compound **7b** was purified by column chromatography, eluting with hexane/EtOAc (9.6:0.4): 86% yield; yellow solid; mp 104−106 °C; IR (KBr) v 2925, 1674, 1449, 1291, 756 cm^{-1}; ^{1}H NMR (300 MHz, CDCl$_3$) δ 3.89 (s, 3H), 3.93 (s, 6H), 6.53 (d, 1H, $J = 16.2$ Hz), 6.79 (s, 1H), 7.18 (d, 1H, $J = 3.77$ Hz), 7.34 (d, 2H, $J = 8.5$ Hz), 7.41−7.46 (m, 3H), 8.29 (d, 1H, $J = 13.6$ Hz); ^{13}C NMR (75 MHz, CDCl$_3$) δ 56.1, 61.0, 61.1, 106.4, 121.9, 123.7, 127.8, 128.4, 128.9, 133.9, 135.4, 136.1, 137.0, 138.3, 145.2, 152.1, 153.0; ESI MS (m/z) 376 (M + H); HRMS (ESI) (m/z) calcd for C$_{19}$H$_{19}$ClNO$_5$, 376.0875, found, 376.0867.

1,2,3-Trimethoxy-4-(4-methylstyryl)-5-((E)-2-nitrovinyl)benzene (7c). Following general procedure B, compound **7c** was purified by column chromatography, eluting with hexane/EtOAc (9.6:0.4): 93% yield; yellow solid; mp 102−105 °C; IR (KBr) v 2935, 1625, 1588, 1487, 1329, 1262, 1124, 962 cm^{-1}; ^{1}H NMR (300 MHz, CDCl$_3$) δ 2.36 (s, 3H), 3.84 (s, 3H), 3.89 (s, 3H), 3.92 (s, 3H), 6.52 (d, 1H, $J = 16.4$ Hz), 6.79 (s, 1H), 7.11−7.21 (m, 3H), 7.37 (d, 2H, $J = 7.93$ Hz), 7.48 (d, 1H, $J = 13.5$ Hz), 8.30 (d, 1H, $J = 13.5$ Hz); ^{13}C NMR (75 MHz, CDCl$_3$) δ 21.2, 56.1, 60.9, 61.0, 106.3, 120.2, 123.6, 126.6, 128.8, 129.4, 134.1, 136.9, 137.6, 138.3, 138.5, 145.2, 152.0, 152.7; ESI MS (m/z) 356 (M + H); HRMS (ESI) (m/z) calcd for C$_{20}$H$_{22}$NO$_5$, 356.1497, found, 356.1481.

2-(2,3,4-Trimethoxy-6-((E)-2-nitrovinyl)styryl)naphthalene (7d). Following general procedure B, compound **7d** was purified by column chromatography, eluting with hexane/EtOAc (9.7:0.3): 91% yield; yellow solid; mp 101−103 °C; IR (KBr) v 2932, 1621, 1588, 1493, 1330, 1243, 1130, 1034, 958 cm^{-1}; ^{1}H NMR (300 MHz, CDCl$_3$) δ 3.89 (s, 3H), 3.94 (s, 6H), 6.75 (d, 1H, $J = 16.2$ Hz), 6.81 (s, 1H), 7.37 (d, 1H, $J = 16.2$ Hz), 7.42−7.55 (m, 3H), 7.70−7.88 (m, 5H), 8.37 (d, 1H, $J = 13.4$ Hz); ^{13}C NMR (75 MHz, CDCl$_3$) δ 56.2. 61.0, 106.4, 121.5, 123.2, 123.7, 126.2, 126.4, 127.3, 127.7, 128.1, 128.4, 133.2, 133.5, 134.3, 137.0, 137.7, 138.5, 145.3, 152.1, 152.9; ESI MS (m/z) 390 (M − H); HRMS (ESI) (m/z) calcd for C$_{23}$H$_{22}$NO$_5$, 392.1420, found, 392.1412.

1,2,3-Trimethoxy-4-(4-methoxystyryl)-5-((E)-2-nitrovinyl)benzene (7e). Following general procedure B, compound **7e** was purified by column chromatography, eluting with hexane/EtOAc (9.4:0.6): 91% yield; yellow solid; mp 111−113 °C; IR (KBr) v 2935, 1615, 1493, 1326, 1253, 1174, 1131, 1034, 958 cm^{-1}; ^{1}H NMR (300 MHz, CDCl$_3$) δ 3.85 (s, 6H), 3.92 (s, 6H), 6.51 (d, 1H, $J = 16.3$ Hz), 6.77 (s, 1H), 6.87 (d, 2H, $J = 8.87$ Hz), 7.11 (d, 1H, $J = 16.3$ Hz), 7.39−7.51 (m, 3H), 8.32 (d, 1H, $J = 13.4$ Hz); ^{13}C NMR (75 MHz, CDCl$_3$) δ 55.3, 56.1, 60.9, 61.1, 106.3, 114.1, 119.0, 123.5, 128.0, 128.3, 129.8, 136.8, 137.3, 138.7, 145.2, 152.0, 152.6, 159.8; ESI MS (m/z) 372 (M + H); HRMS (ESI) (m/z) calcd for C$_{20}$H$_{22}$NO$_6$, 372.1447, found, 372.1457.

1,2,3-Trimethoxy-5-((E)-2-nitrovinyl)-4-(3,4,5-trimethoxystyryl)benzene (7f). Following general procedure B, compound **7f** was purified by column chromatography, eluting with hexane/EtOAc (9.2:0.8): 79% yield; yellow solid; mp 121−124 °C; IR (KBr) v 2932, 1616, 1495, 1323, 1254, 1177, 1129, 1031, 963 cm^{-1}; ^{1}H NMR (300 MHz, CDCl$_3$) δ 3.85 (s, 6H), 3.90−3.94 (m, 12H), 6.36 (s, 1H), 6.46 (d, 1H, $J = 16.1$ Hz), 6.68 (s, 2H), 7.12 (d, 1H, $J = 16.1$ Hz), 7.48 (d, 1H, $J = 13.6$ Hz), 8.31 (d, 1H, $J = 13.6$ Hz); ^{13}C NMR (75 MHz, CDCl$_3$) δ 55.8, 56.2, 56.1, 61.0, 61.2, 61.5, 102.2, 103.8, 104.6, 106.4, 119.4, 120.7, 124.4, 125.4, 127.0,

129.9, 137.0, 137.6, 138.5, 153.4; ESI MS (*m/z*) 454 (M + Na); HRMS (ESI) (*m/z*) calcd for $C_{22}H_{25}NO_8Na$, 454.1477, found, 454.1458.

5-(2,3,4-Trimethoxy-6-((E)-2-nitrovinyl)styryl)benzo[d][1,3]dioxole (7g). Following general procedure B, compound **7g** was purified by column chromatography, eluting with hexane/EtOAc (9.5:0.5): 96% yield; yellow solid; mp 136−139 °C; IR (KBr) v 2926, 1625, 1518, 1489, 1330, 1127, 1031, 962 cm^{-1}; ^1H NMR (300 MHz, CDCl$_3$) δ 3.85 (s, 3H), 3.92 (s, 6H), 5.99 (s, 2H), 6.46 (d, 1H, *J* = 16.2 Hz), 6.74−6.81(m, 2H), 6.90 (d, 1H, *J* = 9.6 Hz), 7.03−7.12 (m, 2H), 7.45 (d, 1H, *J* = 13.6 Hz), 8.29 (d, 1H, *J* = 13.6 Hz); ^{13}C NMR (75 MHz, CDCl$_3$) δ 56.1, 60.9, 61.0, 101.2, 105.6, 106.3, 108.4, 119.4, 122.0, 123.5, 125.2, 126.9, 131.4, 136.8, 137.3, 138.5, 145.2, 148.2, 152.0, 152.7; ESI MS (*m/z*) 386 (M + H); HRMS (ESI) (*m/z*) calcd for $C_{20}H_{20}NO_7$, 386.1239, found, 386.1254.

1,2,3-Trimethoxy-5-((E)-2-nitrovinyl)-4-styrylbenzene (7h). Following general procedure B, compound **7h** was purified by column chromatography, eluting with hexane/EtOAc (9.5:0.5): 90% yield; yellow solid; mp 101−103 °C; IR (KBr) v 2928, 1627, 1525, 1486, 1327, 1127, 1030, 962 cm^{-1}; ^1H NMR (300 MHz, CDCl$_3$) δ 3.86 (s, 3H), 3.92 (s, 6H), 6.58 (d, 1H, *J* = 16.6 Hz), 6.79 (s, 1H), 7.21−7.29 (m, 2H), 7.33−7.38 (m, 2H), 7.43−7.51 (m, 3H), 8.32 (d, 2H, *J* = 13.6 Hz);^{13}CNMR (75 MHz, CDCl$_3$) δ 56.1, 61.0, 96.3, 106.5, 117.7, 121.3, 126.8, 127.0, 127.4, 128.4, 128.9, 134.4, 137.2, 137.8, 138.2, 152.7; ESI MS (*m/z*) 364 (M + Na); HRMS (ESI) (*m/z*) calcd for $C_{19}H_{19}NO_5$ Na, 364.1160, found, 364.1151.

2-(4-Bromostyryl)-3,4,5-trimethoxy-1-((E)-2-nitrovinyl)benzene (7i). Following general procedure B, compound **7i** was purified by column chromatography, eluting with hexane/EtOAc (9.5:0.5): 82% yield; yellow solid; mp 108−111 °C; IR (KBr) v 2926, 1622, 1586, 1487, 1324, 1234, 1128, 1031, 964 cm^{-1}; ^1H NMR (300 MHz, CDCl$_3$) δ 3.86 (s, 3H), 3.92 (s, 6H), 6.52 (d, 1H, *J* = 16.3 Hz), 6.78 (s, 1H), 7.23 (d, 1H, *J* = 16.3 Hz), 7.37 (d, 2H, *J* = 8.5 Hz), 7.42 − 7.49 (m, 2H), 7.53 (d, 1H, *J* = 13.4 Hz), 8.28 (d, 1H, *J* = 13.4 Hz); ^{13}C NMR (75 MHz, CDCl$_3$) δ 56.2, 61.0, 61.1, 106.4, 122.0, 122.1, 123.7, 128.1, 131.9, 135.9, 136.2, 137.1, 138.3, 138.5, 145.2, 152.2, 153.0; ESI MS (*m/z*) 420 (M + H); HRMS (ESI) (*m/z*) calcd for $C_{19}H_{19}NO_5Br$, 420.0446, found, 420.0465.

4-(2,3,4-Trimethoxy-6-((E)-2-nitrovinyl)styryl)biphenyl (7j). Following general procedure B, compound **7j** was purified by column chromatography, eluting with hexane/EtOAc (9.6:0.4): 87% yield; yellow solid; mp 136−138 °C; IR (KBr) v 2926, 1623, 1589, 1487, 1328, 1237, 1124, 1035, 962 cm^{-1}; ^1H NMR (300 MHz, CDCl$_3$) δ 3.87 (s, 3H), 3.93 (s, 6H), 6.62 (d, 1H, *J* = 16.4 Hz), 6.79 (s, 1H), 7.26−7.51 (m, 6H), 7.54−7.61 (m, 5H), 8.34 (d, 1H, *J* = 13.6 Hz); ^{13}C NMR (75 MHz, CDCl$_3$) δ 56.1, 61.0, 61.1, 106.4, 121.3, 123.7, 126.9, 127.1, 127.4, 128.0, 128.8, 131.7, 135.9, 137.0, 137.1, 138.5, 140.5, 141.0, 145.2, 152.1, 152.9; ESI MS (*m/z*) 418 (M + H); HRMS (ESI) (*m/z*) calcd for $C_{25}H_{24}NO_5$, 418.1654, found, 418.1662.

2-(3,5-Dimethoxystyryl)-3,4,5-trimethoxy-1-((E)-2-nitrovinyl)benzene (7k). Following general procedure B, compound **7k** was purified by column chromatography, eluting with hexane/EtOAc (9.4:0.6): 90% yield; yellow solid; mp 119−121 °C; IR (KBr) v 2927, 2849, 1724, 1593, 1458, 1334, 1155, 1124, 1064, 961 cm^{-1}; ^1H NMR (300 MHz, CDCl$_3$) δ 3.82 (s, 6H), 3.85 (s, 3H), 3.93 (s, 6H), 6.37 (s, 1H), 6.50 (d, 1H, *J* = 16.2 Hz), 6.61 (d, 2H, *J* = 2.2 Hz), 6.79 (s, 1H), 7.19 (d, 1H, *J* = 16.2 Hz), 7.46 (d, 1H, *J* = 13.5 Hz), 8.30 (d, 1H, *J* = 13.5 Hz); ^{13}C NMR (75 MHz, CDCl$_3$) δ 55.4, 55.8, 61.1, 61.4, 99.0, 102.1, 104.8, 105.6, 119.6, 125.3, 126.9, 136.4, 137.0, 137.5, 138.4, 143.7, 153.0, 161.0; ESI MS (*m/z*) 402 (M + H); HRMS (ESI) (*m/z*) calcd for $C_{21}H_{24}NO_7$, 402.1552, found, 402.1557.

■ ASSOCIATED CONTENT

ⓢ Supporting Information. ^1H NMR and ^{13}C NMR spectra for compounds **6a−k** and **7a−k**. This material is available free of charge via the Internet at http://pubs.acs.org.

■ AUTHOR INFORMATION

Corresponding Authors
*Phone: +91 40 27191715. Fax: +91 40 27160921. E-mail: (B.S.) sreedharb@iict.res.in, (A.A.) anthony@iict.res.in, or (S.V.K.) kalivendi@iict.res.in.

Author Contributions
∥These authors made equal contributions to the work

■ ACKNOWLEDGMENT

■ ABBREVIATIONS USED

EtOAc, ethyl acetate; PBS, phosphate-buffered saline; SRB, sulforhodamine B; DAPI, 4′,6-diamidino-2-phenylindole

■ REFERENCES

(1) Downing, K. H.; Nogales, E. Tubulin and microtubule structure. *Curr. Opin. Cell Biol.* **1998**, *10*, 16−22.

(2) Jordan, A.; Hadfield, J. A.; Lawrence, N. J.; McGown, A. T. Tubulin as a target for anticancer drugs: agents that interact with the mitotic spindle. *Med. Res. Rev.* **1998**, *18*, 259−296.

(3) Jordan, M. A.; Wilson, L. Microtubules as a target for anticancer drugs. *Nat. Rev. Cancer* **2004**, *4*, 253−265.

(4) Hadfield, J. A.; Ducki, S.; Hirst, N.; McGown, A. T. Tubulin and microtubules as targets for anticancer drugs. *Prog. Cell Cycle Res.* **2003**, *5*, 309−325.

(5) Kuppens, I. E. Current state of the art of new tubulin inhibitors in the clinic. *Curr. Clin. Pharmacol.* **2006**, *1*, 57−70.

(6) Signorelli, P.; Ghidoni, R. Resveratrol as an anticancer nutrient: molecular basis, open questions and promises. *J. Nutr. Biochem.* **2005**, *16*, 449−466.

(7) (a) Aggarwal, B. B.; Shishodia, S. Molecular targets of dietary agents for prevention and therapy of cancer. *Biochem. Pharmacol.* **2006**, *71*, 1397−1421. (b) de la Lastra, C. A.; Villegas, I. Resveratrol as an anti-inflammatory and anti-aging agent: mechanisms and clinical implications. *Mol. Nutr. Food Res.* **2005**, *49*, 405−430.

(8) Jazirehi, A. R.; Bonavida, B. Resveratrol modifies the expression of apoptotic regulatory proteins and sensitizes non-Hodgkin's lymphoma and multiple myeloma cell lines to paclitaxel-induced apoptosis. *Mol. Cancer Ther.* **2004**, *3*, 71−84.

(9) (a) Kotha, A; Sekharam, M.; Cilenti, L.; Siddiquee, K.; Khaled, A.; Zervos, A. S.; Carter, B.; Turkson, J.; Jove, R. Resveratrol inhibits Src and Stat3 signaling and induces the apoptosis of malignant cells containing activated Stat3 protein. *Mol. Cancer Ther.* **2006**, *5*, 621−629. (b) Bhardwaj, A.; Sethi, G.; Vadhan-Raj, S.; Bueso-Ramos, C.; Takada, Y.; Gaur, U.; Nair, A. S.; Shishodia, S.; Aggarwal, B. B. Resveratrol inhibits proliferation, induces apoptosis, and overcomes chemoresistance through down-regulation of STAT3 and nuclear factor-κB-regulated antiapoptotic and cell survival gene products in human multiple myeloma cells. *Blood* **2007**, *109*, 2293−2302. (c) Garvin, S.; Ollinger, K.; Dabrosin, C. Resveratrol induces apoptosis and inhibits angiogenesis in human breast cancer xenografts in vivo. *Cancer Lett.* **2006**, *231*, 113−122. (d) Hsieh, T. C.; Wang, Z.; Hamby, C. V.; Wu, J. M. Inhibition of melanoma cell proliferation by resveratrol is correlated with upregulation of quinone reductase 2 and p53. *Biochem. Biophys. Res. Commun.* **2005**, *334*, 223−230. (e) Trincheri, N. F.; Nicotra, G.; Follo, C.; Castino, R.; Isidoro, C. Resveratrol induces cell death in colorectal cancer cells by a novel pathway involving lysosomal cathepsin D. *Carcinogenesis* **2007**, *28*, 922−931.

(10) Notas, G.; Nixi, A. P.; Kampa, M.; Vercauteren, J.; Kouroumalis, E.; Castanas, E. Resveratrol exerts its antiproliferative effect on HepG2

hepatocellular carcinoma cells, by inducing cell cycle arrest, and NOS activation. *Biochim. Biophys. Acta* **2006**, *1760*, 1657–1666.

(11) (a) Lu, J.; Ho, C. H.; Ghai, G.; Chen, K. Y. Resveratrol analog, 3,4,5,4′-tetrahydroxystilbene, differentially induces pro-apoptotic p53/Bax gene expression and inhibits the growth of transformed cells but not their normal counterparts. *Carcinogenesis* **2001**, *22*, 321–328. (b) Sale, S.; Verschoyle, R. D.; Boocock, D.; Jones, D. J.; Wilsher, N.; Ruparelia, K. C.; Potter, G. A.; Farmer, P. B.; Steward, W. P.; Gescher, A. J. Pharmacokinetics in mice and growth-inhibitory properties of the putative cancer chemopreventive agent resveratrol and the synthetic analogue *trans* 3,4,5,4′-tetramethoxystilbene. *Br. J. Cancer* **2004**, *90*, 736–744. (c) Sale, S.; Tunstall, R. G.; Ruparelia, K. C.; Potter, G. A.; Steward, W. P.; Gescher, A. J. Comparison of the effects of the chemopreventive agent resveratrol and its synthetic analog trans 3,4,5,4′-tetramethoxystilbene (DMU-212) on adenoma development in the Apc(Min+) mouse and cyclooxygenase-2 in human-derived colon cancer cells. *Int. J. Cancer* **2005**, *115*, 194–201. (d) Gosslau, A.; Chen, M.; Ho, C. T; Chen, K. Y. A methoxy derivative of resveratrol analogue selectively induced activation of the mitochondrial apoptotic pathway in transformed fibroblasts. *Br. J. Cancer* **2005**, *92*, 513–521.

(12) Kaap, S.; Quentin, I.; Tamiru, D.; Shaheen, M.; Eger, K.; Steinfelder, H. Structure activity analysis of the pro-apoptotic, antitumor effect of nitrostyrene adducts and related compounds. *J. Biochem. Pharmacol.* **2003**, *65*, 603–610.

(13) Kim, J. H.; Kim, J. H.; Lee, J. E.; Lee, J. E.; Chung, I. K. Potent inhibition of human telomerase by nitrostyrene derivatives. *Mol. Pharmacol.* **2003**, *63*, 1117–1124.

(14) Jain, N.; Yada, D.; Shaik, T. B.; Vasantha, G.; Reddy, P. S.; Kalivendi, S. V.; Sreedhar, B. Synthesis and antitumor evaluation of nitrovinyl biphenyls: anticancer agents based on allocolchicines. *Chem. Med. Chem.* **2011**, *6*, 859–868.

(15) Vakifahmetoglu, H.; Olsson, M.; Zhivotovsky, B. Death through a tragedy: mitotic catastrophe. *Cell Death Differ.* **2008**, *15*, 1153–1156.

(16) Kamal, A.; Balakishan, G.; Ramakrishna, G.; Shaik, T. B.; Sreekanth, K.; Balakrishna, M.; Rajender; Dastagiri, D.; Kalivendi, S. V. Synthesis and biological evaluation of cinnamido linked pyrrolo-[2,1-c][1,4]benzodiazepines as antimitotic agents. *Eur. J. Med. Chem.* **2010**, *45*, 3870–3884.

(17) Huber, K.; Patel, P.; Zhang, L.; Evans, H.; Westwell, A. D.; Fischer, P. M.; Chan, S.; Martin, S. 2-[(1-Methylpropyl)dithio]-1*H*-imidazole inhibits tubulin polymerization through cysteine oxidation. *Mol. Cancer Ther.* **2008**, *7*, 143–151.

(18) Kamal, A.; Suresh, P.; Malla Reddy, A.; Kumar, B. A.; Reddy, P. V.; Raju, P.; Tamboli, J. R.; Shaik, T. B.; Jain, N.; Kalivendi, S. V. Synthesis of a new 4-aza-2,3-didehydropodophyllotoxin analogues as potent cytotoxic and antimitotic agents. *Bioorg. Med. Chem.* **2011**, *19*, 2349–2355.

(19) *AutoDock*, version 4.0; http://www.scripps.edu/mb/olson/doc/autodock/.

(20) Ravelli, R. B.; Gigant, B.; Curmi, P. A.; Jourdain, I.; Lachkar, S.; Sobel, A.; Knossow, M. Insight into tubulin regulation from a complex with colchicine and a stathmin-like domain. *Nature* **2004**, *428*, 198–202.

(21) Morris, G. M.; Goodsell, D. S.; Halliday, R. S.; Huey, R.; Hart, W. E.; Belew, R. K.; Olson, A. J. Automated docking using a Lamarckian genetic algorithm and an empirical binding free energy function. *J. Comput. Chem.* **1998**, *19*, 1639–1662.